Journal of proteome research

Article

pubs.acs.org/jpr

Metabolic Phenotyping of Atherosclerotic Plaques Reveals Latent Associations between Free Cholesterol and Ceramide Metabolism in Atherogenesis

Panagiotis A. Vorkas,[†] Joseph Shalhoub,[‡] Giorgis Isaac,[§] Elizabeth J. Want,[†] Jeremy K. Nicholson,[†] Elaine Holmes,[†] and Alun H. Davies*[,‡]

[†]Biomolecular Medicine, Division of Computational and Systems Medicine, Department of Surgery and Cancer, Faculty of Medicine, Imperial College London, London SW7 2AZ, United Kingdom

[‡]Academic Section of Vascular Surgery, Division of Surgery, Department of Surgery and Cancer, Faculty of Medicine, Imperial College London, London W6 8RF, United Kingdom

[§]Pharmaceutical Discovery and Life Sciences, Waters Corporations, Milford, Massachusetts 01757, United States

Supporting Information

ABSTRACT: Current optimum medical treatments have had limited success in the primary prevention of cardiovascular events, underscoring the need for new pharmaceutical targets and enhanced understanding of mechanistic metabolic dysregulation. Here, we use a combination of novel metabolic profiling methodologies, based on ultra-performance liquid chromatography coupled to mass spectrometry (UPLC–MS) followed by chemometric modeling, data integration, and pathway mapping, to create a systems-level metabolic atlas of atherogenesis. We apply this workflow to compare arterial tissue incorporating plaque lesions to intimal thickening tissue (immediate preplaque stage). We find changes in several metabolite species consistent with well-established pathways in atherosclerosis, such as the cholesterol, purine, pyrimidine, and ceramide pathways. We then illustrate differential levels of previously unassociated lipids to atherogenesis, namely, phosphatidylethanolamine-ceramides (*t*-test *p*-values: 3.8×10^{-6} to 9.8×10^{-12}). Most importantly, these molecules appear to be interfacing two pathways recognized for their involvement in atherosclerosis: ceramide and cholesterol. Furthermore, we show that β-oxidation intermediates (i.e., acylcarnitines) manifest a pattern indicating truncation of the process and overall dysregulation of fatty acid metabolism and mitochondrial dysfunction. We develop a metabolic framework that offers the ability to map significant statistical associations between detected biomarkers. These dysregulated molecules and consequent pathway modulations may provide novel targets for pharmacotherapeutic intervention.

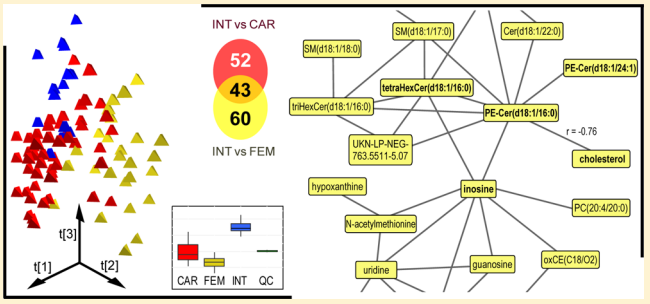

KEYWORDS: *Atherosclerosis, atherogenesis, metabolic profiling, metabonomics, metabolomics, lipidomics, phenotyping, ceramide, phospatidylethanolamine-ceramide, acylcarnitine*

INTRODUCTION

According to estimates by the World Health Organization, atherosclerosis is the number one cause of death in the western world. Most adverse health events associated with atherosclerosis are due to flow limitation because of stenosing plaque or distal embolization due to plaque rupture. Additionally, existing medical management strategies have had limited success in primary prevention, and the scientific community is still struggling to find appropriate doses, drug regimens, and mechanisms of action.[1,2]

Atherosclerosis is a multicentric, multistage, and systemic disease.[3] Cell populations such as vascular smooth muscle cells and leukocytes are known to be important in the manifestation of the disease. These cells participate in microenvironmental interactions in the arterial wall. Intraplaque composition and structure can also be heterogeneous and subject to variation.[4] In order to understand the role of the microenvironment in the etiopathogenesis and progression of the disease, as well as the risk posed by plaque destabilization, there is a need to understand biochemical mechanisms leading to plaque accumulation and instability within the context of a holistic framework. Current omics applications can provide such a holistic representation on a systems level while, at the same time, functioning as hypothesis-generating tools. Metabolic profiling – also referred to as metabonomics or metabolomics, depending on the purpose of the application – is a promising omics strategy for elucidation of pathological mechanisms.[5,6]

Applications of metabolic profiling in cardiovascular disease has been predominately initiated in pilot/feasibility studies[7] and using recognized animal models.[8] Intervention studies conducted using metabolic profiling tools and relating to atherosclerosis are

Received: September 22, 2014
Published: January 7, 2015

DOI: 10.1021/pr5009898
J. Proteome Res. 2015, 14, 1389–1399

Table 1. Patient Demographics of Carotid, Femoral, and Intimal Thickening Groups

	carotid[a]	femoral[a]	intimal thickening[a]
no. of samples	52	26	16
age, median (range)	69 (44−87)	74 (60−91)	69 (58−91)
gender, male (%)	40 (77)	17 (65)	13 (81)
statin therapy (%)	40 (82) {3}	19 (73)	13 (87) {1}
antiplatelet therapy (%)	43 (86) {3}	22 (85)	14 (93) {1}
hypertension (%)	32 (68) {5}	13 (50)	7 (47) {1}
diabetes mellitus (%)	11 (22) {3}	7 (27)	6 (40) {1}
ever smoker (%)	25 (52) {4}	18 (69)	11 (73) {1}
body mass index, median (range)	25.5 (17.4−41.2) {9}	23.0 (21.6−33.3) {13}	25.4 (21.0−47.7) {6}

[a]{ } indicates the number of missing patients.

also reported in the literature.[9,10] Multicenter, large population studies followed, aiming toward the identification of relevant risk factors.[11−13] Currently, in the literature, only a limited number of studies on cardiovascular disease apply metabolic profiling technologies on human tissue[14] or, specifically, atherosclerosis.[15] This dictates the need to emphasize top-down systems biology applications that can provide important biological, mechanistic, and systemic information at the tissue level.

In this study, we adopted a metabolic profiling and molecular biomarker discovery approach combined with computational modeling to study the metabolic changes of the progression from intimal thickening (INT) to stenosing plaque formation from human carotid (CAR) and femoral (FEM) endarterectomy specimens. It is important to address the differences in metabotypes between these two different anatomical locations in the peripheral arterial tree, as they experience differences in biochemical composition and rupture risk.[16−18] Lastly, the use of INT tissue as a control holds several advantages as opposed to the use of normal tissue, including the following: (i) INT, rather than normal tissue, is detected at plaque-prone sites from the early years of a person's life, (ii) it is the immediate stage prior to progression to the lipid-laden stenosing plaque and thus the experimental model can provide a more realistic course of the disease, (iii) normal fresh tissue is difficult to obtain for ethical reasons, and (iv) arterial tissue considered to be normal may contain subclinical and/or macroscopically undetectable disease. To our knowledge, a metabolic profiling characterization of plaques using INT tissue as a control has not been previously reported.

We used ultra-performance liquid chromatography coupled to mass spectrometry (UPLC−MS) in order to identify dysregulated metabolites between the patient groups. Two untargeted UPLC−MS methodologies were applied in order to cover molecules spanning a wide range of physicochemical properties. Highly predictive and cross-validated multivariate statistical models demonstrated commonly dysregulated metabolites from the FEM and CAR when they were individually compared to INT. Moreover, we identify a global metabolic phenotype (metabotype: the multiparametric metabolic responses characterizing a phenotype)[19] of plaque formation, comprising metabolites known to be associated with atherogenesis and, importantly, metabolites indicating the contribution of biological pathways as yet unrecognized for their involvement in atherogenesis. Finally, we developed a framework for mapping significant statistical interactions between metabolites and biological pathways in relation to atherogenesis.

MATERIAL AND METHODS

Patients

Research ethics committee approval (RREC 2989 and RREC 3199) and informed consent were obtained for the collection of endarterectomy specimens. Retrieved samples were stored at −80 °C until the time of dissection and metabolite extraction. The atherosclerotic plaque (> 50% stenosis) tissue samples used in this study were obtained from a total of 78 patients from the Academic Section of Vascular Surgery, Imperial College London: 52 patients underwent carotid endarterectomy (CAR) and 26 patients underwent femoral endarterectomy (FEM). From a proportion of these samples, areas of intimal thickening (INT) were separated from the stenosing plaque segment (9 samples from carotid and 7 samples from femoral tissue). INT tissue, found at the proximal and distal extents of stenosing atheroma samples, served as control tissue in this study. Patients' clinical characteristics are detailed in Table 1.

Tissue Dissection and Metabolite Extraction

Parts of plaque tissue, and intima tissue adjacent to plaque, were dissected, and sections were harvested for metabolite extraction. Tissue section weights were in the range of 153−416 mg. Tissue samples were loaded into appropriate bead-beating tubes (Percellys Steel-Kit, Germany) along with steel beads and subjected to tissue lysis and metabolite extraction. A consecutive extraction protocol was applied with aqueous extraction followed by organic as previously described (Vorkas et al; in press).[20]

Ultra-Performance Liquid Chromatography−Mass Spectrometry

Detailed UPLC−MS protocols have been previously described (Vorkas et al; in press).[20] Briefly, aqueous extracts were subjected to hydrophilic interaction (liquid) chromatography (HILIC) UPLC−MS analysis, whereas organic extracts were subjected to a lipid profiling reversed-phase (RP) UPLC−MS analysis. A quality control pooled sample (QC) was injected every 10 samples in order to assess instrument stability and feature reproducibility through the run.[21] Data extraction for both analyses was conducted using MarkerLynx XS (Waters Inc., v. 4.1) software. Data extraction comprised peak picking and grouping followed by total area normalization.

Statistical Analysis

Multivariate data analysis (MVDA) for UPLC−MS data was conducted using SIMCA-P+ (v. 12.0.1.0; Umetrics). Principal components analysis (PCA) and orthogonal projection to latent structures-discriminant analysis (OPLS-DA) were applied to the processed Pareto-scaled data. Model validation was carried out using CV-ANOVA testing.[22]

DOI: 10.1021/pr5009898
J. Proteome Res. 2015, 14, 1389−1399

In order to extract putative biomarkers from the UPLC−MS data, metabolite features with a correlation coefficient (p_{corr}, correlation coefficient that refers to correlation of samples to disease classes) greater than 0.5 in absolute value were chosen ($p < 0.001$). These features were further subjected to two-tailed *t*-test, assuming unequal variance with a threshold of $p < 0.05$,[23,24] and fold-change comparison using their median values. Features were reported as significant and structurally identified if (1) both p_{corr} and *t*-test *p*-value met the thresholds, (2) they were reproducible through the run, with a coefficient of variation (CV%) in the QC samples of less than 30%, and (3) they passed the chromatographic peak shape assessment. A brief flowchart of the conditions that a feature had to pass in order to be considered statistically significant and robust is illustrated in Supporting Information Figure S1.

Structural Assignment of Candidate Biomarkers

Elucidation and validation of the molecular structure of significant features is critical for the process of biological interpretation. Here, we have used multiple methods to elucidate and validate the molecular structures of candidate biomarkers. Structural elucidation of significant features was initially guided by matching accurate *m/z* measurements to metabolites from available online databases.[25−27] The extraction phase (i.e., aqueous or organic) along with retention time also contributed to narrowing putative matches. In some cases, isotopic patterns and an in-house developed library were used to provide additional confirmation.[20,28] Furthermore, UPLC−MS^E and UPLC−MS/MS data were used for structural elucidation. For lipid profiling analyses, MS^E data were collected for every sample throughout the run, whereas for the HILIC−UPLC−MS analyses, MS^E data were collected only on pooled samples (QCs) at the end of the run. The conditions described for each run were identical to those used for MS/MS analysis, either conducted using data-dependent acquisition (DDA) or by targeting specific ions. MS/MS data were collected with collision energy ramping from 30 to 50 eV for lipid profiling and 20 to 40 eV for HILIC analysis. Supporting Information Tables S1 and S2 present all of the features detected with statistical significance, and structurally assigned metabolites were allocated a level of assignment, according to whether they were matched to (1) accurate mass, (2) accurate mass and tandem MS to *in silico* fragmentation pattern, (3) tandem MS from databases or literature, (4) authentic standard matched to retention time, and (5) authentic standard matched to MS/MS spectrum. Unknown or tentative assignments are also stated.

Additional methods were further employed in order to validate elucidated molecular structures, providing an extra level of confidence. These methods proved useful for revealing biological associations between metabolites using pathway mapping and mathematical pairwise correlations (*r*). The detailed methodological procedures are described in the following paragraphs.

Analytical Standards

Standards were of analytical grade with typical purity >99%. A detailed description is presented in the Supporting Information.

Correlation Network Analysis

Spearman pairwise correlation coefficients (*r*) between pairs of metabolites (detected as being different between the groups with statistical significance), along with two-tailed significance tests (*p*-value), were calculated using R (2.13.2) programming language. When a metabolite was detected as being statistically different using more than one method or polarity mode, the condition under which the metabolite demonstrated the lowest

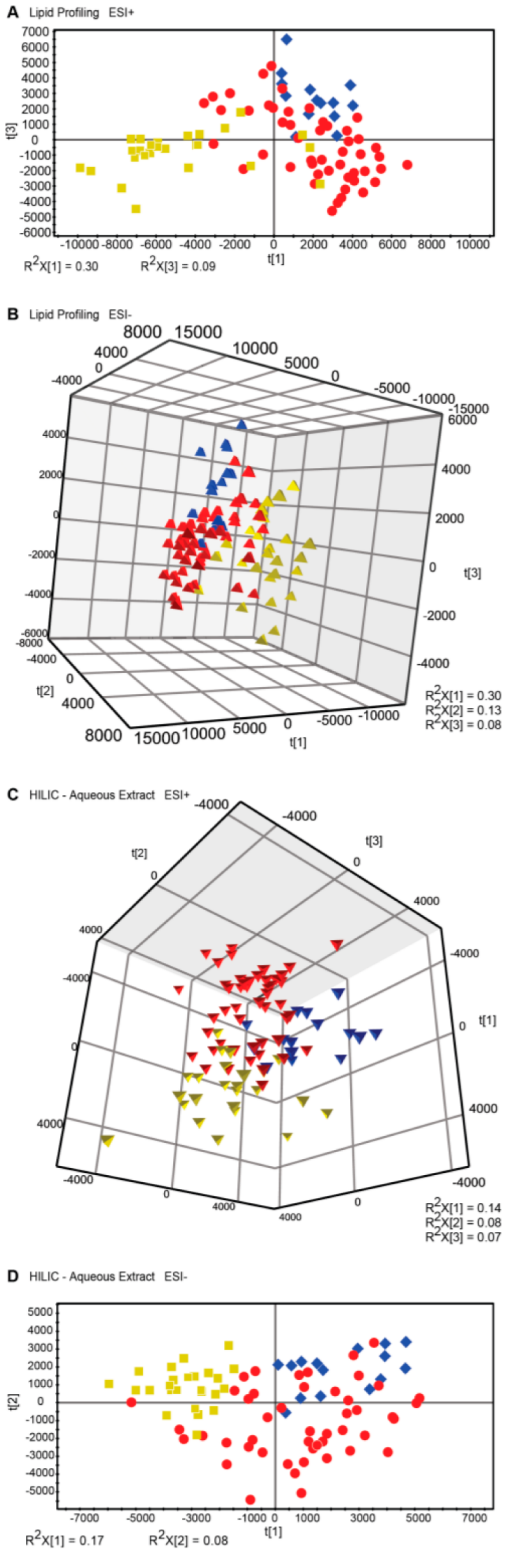

Figure 1. Scores plots of principal components analysis (PCA) of the tissue extracts (blue, intimal thickening tissue; red, carotid plaques; yellow, femoral plaques). (A) Positive mode (ESI^+) lipid profiling using reversed-phase ultra-performance liquid chromatography coupled to mass spectrometry (RP−UPLC−MS); (B) negative mode (ESI^-) lipid profiling using RP−UPLC−MS; (C) positive mode (ESI^+) analysis of aqueous extracts using hydrophilic interaction ultra-performance liquid chromatography coupled to mass spectrometry (HILIC−UPLC−MS) analysis; (D) negative mode (ESI^-) analysis of aqueous extracts using HILIC−UPLC−MS analysis.

DOI: 10.1021/pr5009898
J. Proteome Res. 2015, 14, 1389−1399

Table 2. Summary of Model Characteristics from OPLS-DA Multivariate Statistical Analyses of Data Obtained from All Analyses and Electrospray Ionization Polarity Modes[a]

groups	analysis	polarity mode	components (pred + orthog)	R^2X	R^2Y	Q^2Y	CV-ANOVA
CAR vs INT	LP	Pos	1 + 1	0.280	0.609	0.432	1.02×10^{-6}
		Neg	1 + 2	0.412	0.786	0.502	3.99×10^{-7}
	HL	Pos	1 + 0	0.131	0.496	0.356	1.48×10^{-6}
		Neg	1 + 1	0.215	0.721	0.467	2.31×10^{-7}
FEM vs INT	LP	Pos	1 + 1	0.423	0.861	0.755	2.82×10^{-10}
		Neg	1 + 1	0.383	0.834	0.746	5.52×10^{-10}
	HL	Pos	1 + 1	0.209	0.895	0.703	4.54×10^{-9}
		Neg	1 + 0	0.193	0.846	0.797	1.59×10^{-13}

[a]CAR, carotid plaque arterial tissue; FEM, femoral plaque arterial tissue; INT, intimal thickening arterial tissue; LP, lipid profiling; HL, HILIC analysis of aqueous extracts; Pos, positive polarity mode; Neg, negative polarity mode; pred, predictive components; orthog, orthogonal component; CV-ANOVA, cross-validation ANOVA testing of residual values from cross-validation testing.

CV% was preferred for representation. For network visualization, CytoScape (v.3.0.0-beta1) software was used.

Metabolite Mapping

Metabolite mapping was conducted using the KEGG database.[29] A number of metabolites were also mapped based on literature findings.

Venn Diagrams

Venn diagrams of detected metabolites per method and polarity mode were constructed using online available software (http://bioinfogp.cnb.csic.es/tools/venny/).

RESULTS AND DISCUSSION

Metabolic Profiling Reveals the Metabotype of the Lipid-Laden Plaque

Complex diseases such as atherosclerosis with mosaic etiological factors necessitate a systemic approach for their mechanistic understanding and for optimization of therapeutic targets. Advances in UPLC−MS technology,[30] resulting in the ability to profile thousands of metabolites reliably in biological matrices, present opportunities for continuous discovery. This can be the case even in a widely studied disease such as atherosclerosis. We applied two UPLC−MS methodologies, covering a range of metabolites with substantial diversity of physicochemical properties, to characterize metabolic alterations from the intimal thickening stage to the lipid-laden stenosing plaque.

The metabotype of atherogenesis could function as a metabolic atlas to guide future studies on atherosclerosis. In order to accomplish this, we first applied principal components analysis (PCA) to map the UPLC−MS profiles (Figure 1). We observed a clear separation between samples from INT and plaque lesions from the CAR and FEM locations. This indicated distinct metabotypes of human INT and advanced plaque lesions. The samples from CAR and FEM tissue also formed distinct groups, with the CAR phenotype being metabolically closer to INT rather than the FEM plaque tissue. Conversely, INT tissue, although collected from the carotid and femoral arterial bifurcations, did not present metabolic origin-related differences.

We further applied orthogonal projection to latent structure-discriminant analysis (OPLS-DA) in order to optimally extract candidate metabolites responsible for differentiating between the intimal thickening tissue and the two atherosclerotic plaque groups. OPLS-DA was performed in a pairwise fashion, wherein CAR and FEM were compared individually with the INT tissue group. Both models displayed high predictive values, indicating distinctive metabotypes for INT versus plaque tissue; model diagnostics indicated that the models were robust and predictive (Table 2). Cross-validation ANOVA testing (CV-ANOVA) was applied as a significance test of the OPLS models (Table 2).[22] Cross-validated scores plots of the analyzed samples are shown in Supporting Information Figure S2.

The constructed multivariate models, in conjunction with univariate statistical analysis, enabled highly significant features to be revealed. We assigned >150 unique metabolite structural identities for features that were found to be statistically significant in differentiating between tissue groups (Figures 2 and 3 and Supporting Information Tables S1 and S2). Lipid moieties classified into 5 different lipid classes and 17 subclasses, according to the proposed classification system,[31] were structurally assigned. A large number of the metabolites were identified as being statistically significant in more than one UPLC−MS analysis or polarity mode.

The common metabolites detected with statistical significance in both CAR and FEM (Figure 4) after individual comparisons to controls follow the same trends in both disease locations. This common signature of perturbed metabolites can provide a good overview of the basis of metabolic dysregulation leading to plaque formation and will be the main focus of analysis and discussion in the following paragraphs. Several metabolites demonstrated statistical significance with only one of the tested plaque locations. However, a detailed comparison between the plaque tissues from the two anatomical locations goes beyond the scope of this article.

Higher Levels of Free Cholesterol and Cholesterol Derivatives in Plaques Provide Confidence in Our Experimental Design

Free cholesterol (Cho) and cholesterol derivatives are well-established risk factors for atherogenesis.[32] Accumulation of cholesteryl esters (CE) is considered to be a major contributor to plaque formation, whereas Cho accumulates in advanced atherosclerotic plaques.[33] In this study, we detected Cho with higher intensities in both CAR and FEM tissue as compared to that in INT (Figures 4D and 5A,B). Moreover, several oxidized cholesteryl ester (oxCE) moieties were detected with higher intensities in plaques, with higher statistical significance and fold-change than that of Cho. Additional involvement of the Cho pathway is shown in FEM, where cholesterol sulfate was also found to be higher by 2-fold compared with INT samples. Although the detection of higher levels of Cho and derivatives does not constitute a novel finding, it does provide further validation of our experimental design and findings.

DOI: 10.1021/pr5009898
J. Proteome Res. 2015, 14, 1389−1399

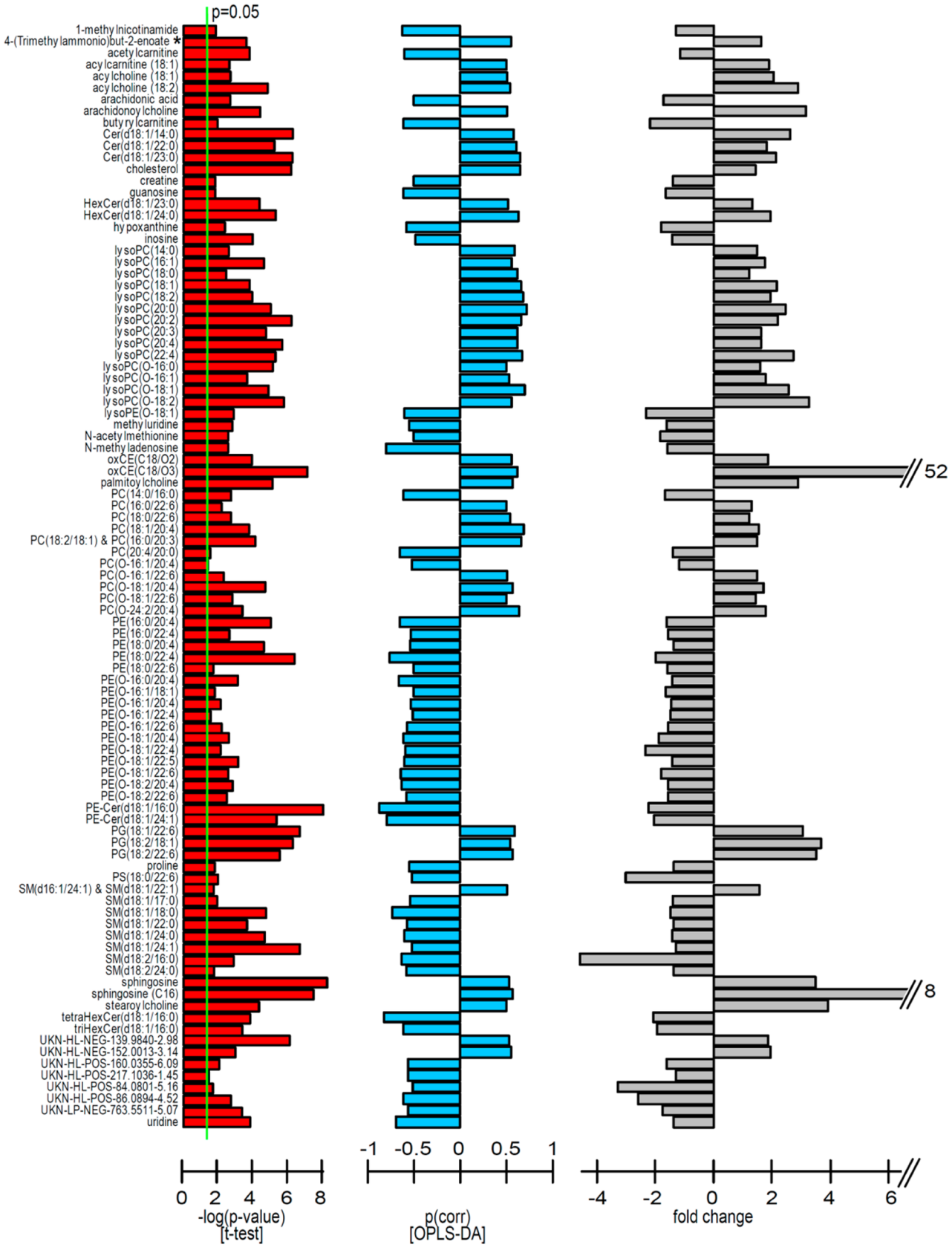

Cer: ceramide, HexCer: hexosylceramide, oxCE: oxidized cholesterol ester, PC: phosphatidylcholine, PE: phosphatidylethanolamine, PE-Cer: phosphatidylethanolamine-ceramide, PG: phosphatidylglycerol, PS: phosphatidylserine, SM: sphingomyelin, UKN: unknown, *: tentative assignment

Figure 2. Statistically significant metabolite changes between carotid plaques and intimal thickening tissue. Bar plots represent, from left to right, −log(p-value) of t-test (two-tailed; assuming unequal variance), p_{corr} obtained from orthogonal projection to latent structures-discriminant analysis (OPLS-DA), and fold change.

DOI: 10.1021/pr5009898
J. Proteome Res. 2015, 14, 1389−1399

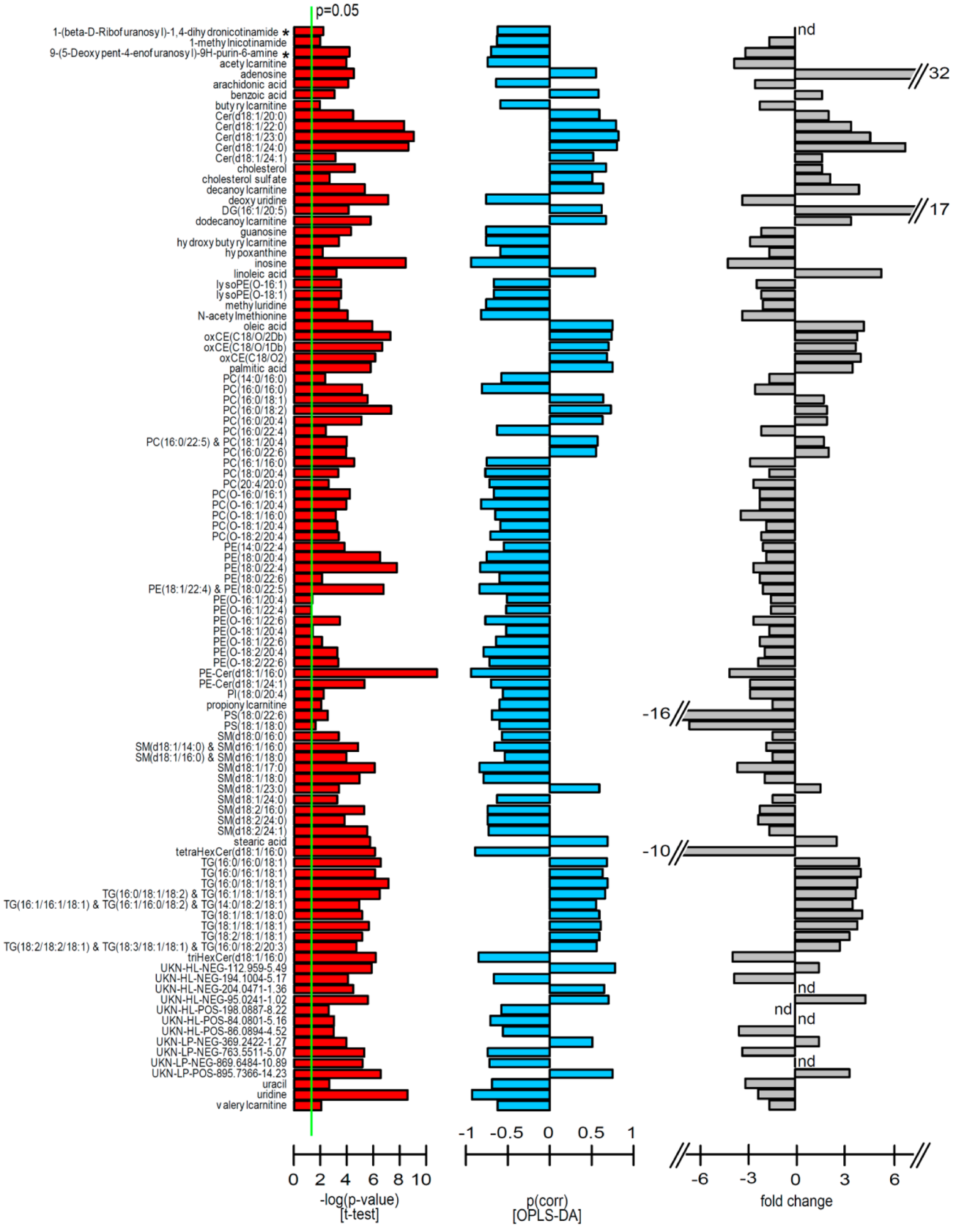

Cer: ceramide, DG: diglyceride, HexCer: hexosyl-ceramide, oxCE: oxidized cholesterol ester, PC: phosphatidylcholine, PE: phosphatidylethanolamine, PE-Cer: phosphatidylethanolamine-ceramide, PI: phosphatidylinositol, PS: phosphatidylserine, SM: sphingomyelin, TG: triglyceride, UKN: unknown Db: number of fatty chain double bonds, nd: not determined (divided by zero), *: tentative assignment.

Figure 3. Statistically significant metabolite changes between femoral plaques and intimal thickening tissue. Bar plots represent, from left to right, −log(p-value) of t-test (two-tailed; assuming unequal variance), p_{corr} obtained from orthogonal projection to latent structures-discriminant analysis (OPLS-DA), and fold change.

DOI: 10.1021/pr5009898
J. Proteome Res. 2015, 14, 1389−1399

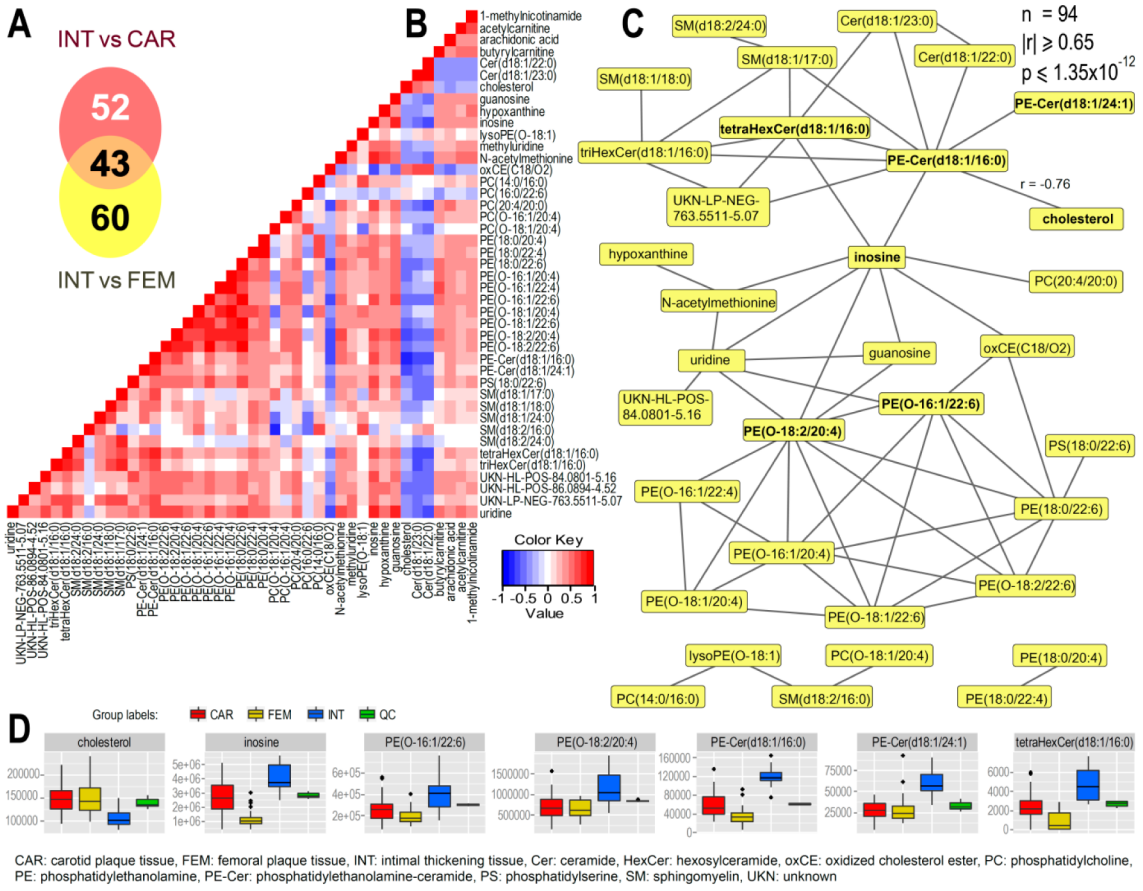

Figure 4. Analysis of metabolites found to be commonly dysregulated with statistical significance after separate comparisons of carotid (CAR) and femoral (FEM) plaques to intimal thickening tissue (INT). (A) Venn diagram demonstrating the number of unique and commonly dysregulated metabolites between the two anatomical locations. These metabolite entities were deemed to be significant after individual comparisons to INT. (B) Correlation matrix of metabolite pairs using Spearman correlation. (C) Correlation network of metabolite pairs found to have a Spearman correlation of absolute value ≥ 0.65. (D) Box plots of highlighted metabolites from the correlation network. These metabolites are considered to be important due to the central role (hubs) in the network or prior knowledge of importance in the disease studied according to the literature.

All oxCEs detected in higher levels were esterified exclusively with 18C fatty acyl chains; these chains were detected with incorporating 1−3 oxygen atoms. Free radicals have been suggested to promote the production of oxCE.[34,35] Lipid oxidation is known to be caused by reactive oxygen species (ROS) and affects unsaturated fatty acids as well as cholesteryl esters and Cho itself.[35] Lipid oxidation can ultimately result in an oxidation chain reaction and cell membrane damage[34] and has a well-recognized role in the progression of atherogenesis.[33] Moreover, oxCEs are known to contribute to foam cell formation,[36] since macrophages are less efficient for oxCE degradation.[37] The structures of oxCE moieties identified in this study are in concordance with published literature.[38]

Dysregulation of Purine and Pyrimidine Pathways

Using HILIC analysis, we observed a large number of metabolites from the purine and pyrimidine pathways detected in lower intensities in both plaque groups. These include inosine (Figure 4D), uridine, hypoxanthine, guanosine, and methyluridine (Figures 2 and 3 and Supporting Information Tables S1 and S2). These results provide additional validity to the current study, since they are well-established for their involvement in atherosclerosis.[39,40] Triphosphates of adenosine and uridine are released from endothelial cells in response to sheer stress.[41] Purines and pyrimidines control vascular tone[40,41] in a process related to hypoxia, and a number of them, such as adenosine and inosine, are known for their anti-inflammatory effects.[42,43] Purines and pyrimidines are essential for cell proliferation,[44] and their inhibition can lead to apoptosis.[44] Metabolites of these pathways are components or precursors of RNA and DNA.

The Ceramide Pathway Suffers Extensive Homeostatic Loss in Plaque Tissue

Dysregulation of the Cer pathway was detected with several altered metabolites (Supporting Information Figure S3). This was evident by the global reduction in the levels of a number of sphingomyelin (SM) moieties, which, together with the detected higher levels of ceramides (Cer) (Figures 2 and 3) in the diseased groups, indicated involvement of the sphingomyelinase (SMase) enzyme. SMase catalyzes the production of Cer by hydrolysis of the phosphoesteric bond of the phosphocholine headgroup of SMs and has been previously shown to be involved in atherosclerosis.[45] The Cer pathway is known for its involvement in atherosclerosis,[46] with a role in apoptosis,[47] and connections to pro-inflammatory factors, ROS and nitric oxide.[46]

We also found that glycosphingolipids, another sphingolipid subclass, were dysregulated. Studies detecting glycosphingolipid involvement in atherogenesis have existed in the literature for 40 years.[48] They have been implicated as signaling molecules in vascular cell proliferation under oxidative conditions[45] as well as for platelet activation and adhesion to the vessel wall.[49] In the present study, tetrahexosylceramide (tetraHexCer) (Figure 4D)

DOI: 10.1021/pr5009898
J. Proteome Res. 2015, 14, 1389−1399

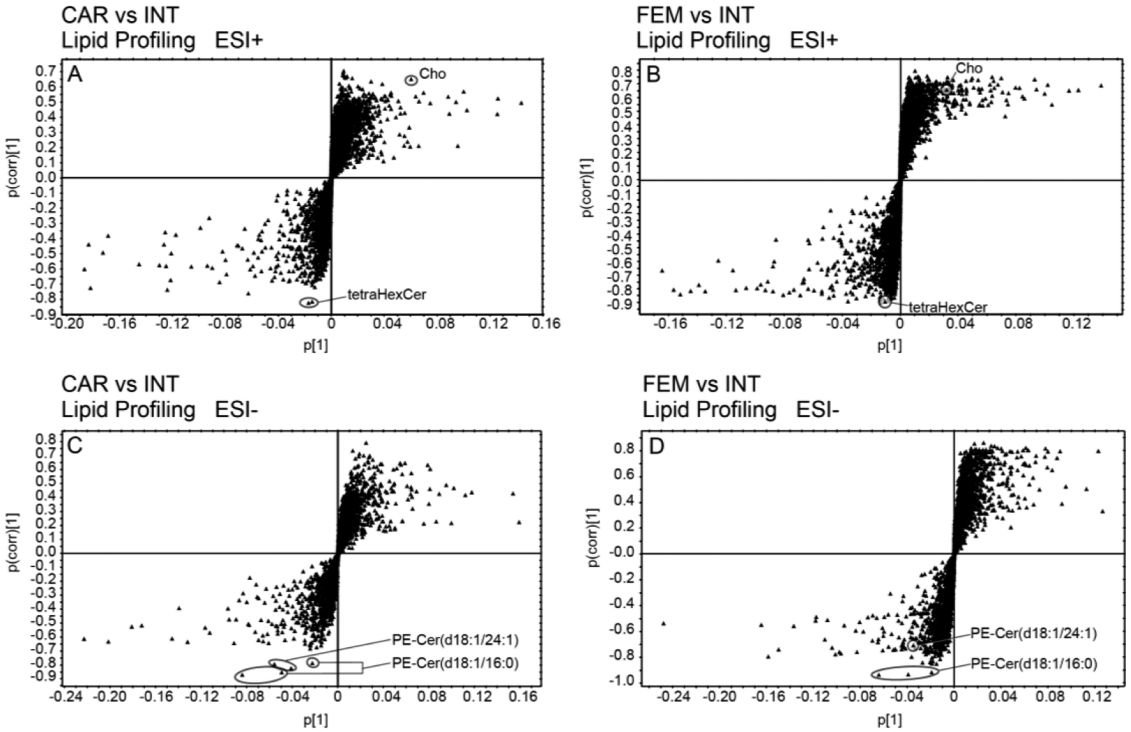

Figure 5. S-plots obtained from orthogonal projection to latent structures-discriminant analysis (OPLS-DA) of the data obtained from the organic tissue extracts. Plots highlight statistically and/or biologically significant metabolites. (A) Positive mode (ESI+) lipid profiling using reversed-phase ultra-performance liquid chromatography coupled to mass spectrometry (RP-UPLC-MS) of the comparison between carotid plaque tissue (CAR) organic extracts and intimal thickening (INT). (B) Positive mode lipid profiling using RP-UPLC-MS of the comparison between femoral plaque tissue (FEM) organic extracts and INT. (C) Negative mode (ESI−) lipid profiling using RP-UPLC-MS of the comparison between CAR organic extracts and INT. (D) Negative mode lipid profiling using RP-UPLC-MS of the comparison between FEM organic extracts and INT.

and trihexosylceramide (triHexCer) were detected in lower intensities in plaques and in the form of d18:1/16:0. Specifically, tetraHexCer was detected with strong statistical significance in both disease locations (Figures 2, 3, and 5A,B).

Phosphatidylethanolamine-Ceramides: New Candidate Biomarkers in Atherogenesis

Phosphatidylethanolamine-ceramides (PE-Cer) are also members of the Cer pathway. To our knowledge, PE-Cers have neither been previously investigated in the context of atherosclerotic plaque formation nor directly related to any other human disease. In this study, using well-validated multivariate models, the levels of two PE-Cers were detected to be highly correlated to the plaque groups ($|p_{corr}|$ = 0.70−0.94) (Figures 2, 3, and 5C,D) and with *t*-test *p*-values 3.8×10^{-6} to 9.8×10^{-12} (Figures 2 and 3). The structures of the two detected PE-Cers were elucidated using MS/MS experiments and were identified as PE-Cer(d18:1/16:0) and PE-Cer(d18:1/24:1). MS/MS spectra used for structural elucidation along with parent and fragment ion structures are presented in Supporting Information Figure S4.

PE-Cer involvement in the progression of plaque formation was evident in plaques from both anatomical locations (CAR and FEM), indicating a common basis for disease progression (Figure 4D). PE-Cers are found only in trace concentrations in mammalian cells.[50] A selective synthase, namely, sphingomyelinase synthase-related (SMSr),[51] also referred to as sterile alpha motif domain containing 8 (SAMD8) or CDP-ethanolamine:N-acylsphingosine ethanolaminephosphotransferase,[29] is responsible for PE-Cer synthesis by transferring the phosphoethanolamine group from phospatidylethanolamines (PE) to Cers.[29] This enzyme has been reported to be essential to ceramide homeostasis in experiments conducted in human cells.[51]

The inverse correlation (Figure 4B,C) of PE-Cer to Cer is in concordance with the aforementioned biochemical reaction (Supporting Information Figure S3). However, PEs did not share the same trend as Cer. On the contrary, PEs had a high positive correlation to PE-Cers. PE-Cers also showed high correlations with members of the purine and pyrimidine pathways, namely, inosine, uridine, guanosine, hypoxanthine, and methyluridine (Figure 4B,C). Specifically, when metabolites commonly dysregulated in both CAR and FEM were assembled in a correlation network (Figure 4C), inosine (Figure 4D) was the metabolite demonstrating a central role (hub) in the network and connecting PE-Cer(d18:1/16:0) and tetraHexCer(d18:1/16:0), both metabolites of the Cer pathway, with PEs, oxCE, and pyrimidine and purine pathways.

High observed correlations between PE-Cers and other members of the ceramide pathway are to be expected. However, correlations of PE-Cers to tetraHexCer were generally higher than triHexCer and at the same level as with Cers. This should be further explored since it is not consistent with canonical pathways (Supporting Information Figure S3), but it is indicative of a more direct association between PE-Cers and tetraHexCers.

Phosphatidylethanolamine-Ceramides Link the Ceramide Pathway to Free Cholesterol

Efforts have previously been made to connect the Cer pathway to Cho,[52,53] since some degree of association has been shown

DOI: 10.1021/pr5009898
J. Proteome Res. 2015, 14, 1389−1399

between them,[54] particularly with respect to their proposed involvement in atherosclerosis.[46] Here, we identified strong inverse pairwise correlations of PE-Cers to Cho, the highest found correlations to Cho of any metabolite detected with statistical significance. Figure 3B,C and Supporting Information Figure S5 illustrate this high correlation of Cho to PE-Cer(d18:1/16:0) ($r = -0.76$; $p = 2.9 \times 10^{-18}$) and PE-Cer(d18:1/24:1) ($r = -0.61$; $p = 2.2 \times 10^{-10}$). The remaining detected Cer pathway metabolites showed $|r| < 0.50$, consistent with a less direct association. Therefore, PE-Cers, and predominantly PE-Cer(d18:1/16:0), have potential to be the missing link from the association of Cho to the Cer pathway.

Macrophage apoptosis is an established feature of atherogenesis,[55] and Cho has been previously shown to have the ability to induce apoptosis in macrophages.[56] Additionally, it has been recently shown that the SMSr enzyme functions as a suppressor of ceramide-induced mitochondrial apoptosis.[57] We therefore propose that Cho promotes apoptosis through reduction of the activity of the SMSr enzyme. Nonetheless, the association between PE-Cers and Cho may be of translational potential in the context of targeting the PE-Cer reaction in order to reduce the lipid load within the atherosclerotic plaque as well as for use as a diagnostic marker of active and advancing atherogenesis.

Truncation of β-Oxidation and Consumption of Unsaturated Lipids Suggests Dysregulation of Metabolic Oxidation

Global perturbations of acylcarnitine (AcC; carnitine ester) metabolism was manifested in plaque tissue. Specifically, we observed that, while levels of short-chain AcCs were detected with fold changes as low as −2.2 in CAR and FEM, medium- and long- (≤16C) chain AcC levels were increased in CAR and FEM, respectively (Figures 2 and 3). AcCs are involved in the translocation of fatty acyl chains through the mitochondrial membrane. Our findings implicate mitochondrial metabolism, specifically, β-oxidation, in plaque development. We also observed a reduction in lipid species with highly unsaturated FACs in plaque tissue (Figures 2−4). The accumulation of medium- and long-chain AcCs led us to hypothesize that β-oxidation is truncated, consequently reducing the production of short-chain AcCs and leading to the recruitment of unsaturated FACs in order to compensate metabolic requirements. These findings are indicative of dysregulations in metabolic oxidation.[58] It is known that β-oxidation and oxidative conditions, in general, are linked to inflammation.[59] Additionally, the aforementioned mitochondrial apoptosis has been previously associated with reduction of β-oxidation.[60] Oxidative stress and mitochondrial dysfunction are known to be involved in the manifestation of atherosclerosis.[61,62]

CONCLUSIONS

Atherosclerosis is a systemic, multicentric, and multistage disease and should be put into context as such. In this study, we first present the metabotype of atherogenesis, providing more than 150 assigned metabolites. Dysregulated metabolites were identified using a diagnostic combination of multivariate and univariate statistics. We further highlight new biochemical pathways suggested as being involved in metabolic perturbations responsible for the progression from intimal thickening to stenosing atherosclerotic plaque. The choice of intimal thickening tissue as the control group, along with metabolites detected with trends in concordance with the published literature and well-established risk factors, namely, Cho and oxCEs,[32,38] purines and pyrimidines, and the Cer pathways, provide additional confidence in our findings.

We observed interruption of β-oxidation in atherosclerotic plaque tissue, as inferred by the differential intensities of acylcarnitines, along with the global recruitment of highly unsaturated fatty acids and formation of oxCEs. Additionally, we identified a novel candidate biomarker in atherogenesis, namely, phosphatidylethanolamine-ceramide, which demonstrated high statistical association with cholesterol. These findings support the identification of novel potential pharmaceutical targets, aiming toward reducing the plaque lipid load, a current and unmet need of the medical community. Additionally, molecules manifesting altered levels could function as indicators of current and profound atherogenesis with potential applications in guiding treatment. Taken together, our findings convey the systemic metabolic signature of atherosclerotic plaque formation, and the identified associations allow observations of mechanistic and translational potential.

ASSOCIATED CONTENT

Supporting Information

Detailed description of analytical standards used in this study. Figure S1: The workflow of conditions a metabolite feature has to fulfill in order to be considered statistically significant and robust. Figure S2: CV-scores plots from OPLS-DA of tissue extracts. Figure S3: A scheme demonstrating the differentially detected ceramide pathway metabolites. Figure S4: MS/MS spectra of the two phosphatidylethanolamine-ceramides (PE-Cer) moieties. Figure S5: Charts illustrating the correlation of phosphatidylethanolamine-ceramides (PE-Cer) to free cholesterol (Cho). Table S1. List of statistically significant and structurally assigned metabolites for the comparison of CAR to INT. Table S2: List of statistically significant and structurally assigned metabolites for the comparison of the FEM to INT. This material is available free of charge via the Internet at http://pubs.acs.org.

AUTHOR INFORMATION

Corresponding Author

*Tel: +44 (0)20 3311 7309. E-mail: a.h.davies@imperial.ac.uk.

Notes

The authors declare no competing financial interest.

ACKNOWLEDGMENTS

The study was funded by the Royal Society of Chemistry (RSC) (grant no. 09/G31C). Additional support was received by the National Institute for Health Research (NIHR) Biomedical Research Centre based at Imperial College Healthcare NHS Trust and Imperial College London. The views expressed are those of the author(s) and not necessarily those of the NHS, the NIHR or the Department of Health. P.A.V. acknowledges the RSC for supporting his Ph.D. studentship. J.S. acknowledges the Royal College of Surgeons of England Research Fellowship Scheme, Circulation Foundation, Rosetrees Trust, Graham Dixon Trust and Peel Medical Research Trust for supporting his Ph.D. studentship. E.J.W. would like to acknowledge Waters Corporation for her funding. Many thanks to Gabriel N. Valbuena for providing suggestions on manuscript preparation.

DOI: 10.1021/pr5009898
J. Proteome Res. 2015, 14, 1389−1399

REFERENCES

(1) Tian, J.; Gu, X.; Sun, Y.; Ban, X.; Xiao, Y.; Hu, S.; Yu, B. Effect of statin therapy on the progression of coronary atherosclerosis. *BMC Cardiovasc. Disord.* **2012**, *12*, 70.

(2) Alexopoulos, N.; Melek, B. H.; Arepalli, C. D.; Hartlage, G. R.; Chen, Z.; Kim, S.; Stillman, A. E.; Raggi, P. Effect of intensive versus moderate lipid-lowering therapy on epicardial adipose tissue in hyperlipidemic post-menopausal women: a substudy of the BELLES trial (Beyond Endorsed Lipid Lowering with EBT Scanning). *J. Am. Coll. Cardiol.* **2013**, *61*, 1956−61.

(3) Shalhoub, J.; Sikkel, M. B.; Davies, K. J.; Vorkas, P. A.; Want, E. J.; Davies, A. H. Systems biology of human atherosclerosis. *Vasc. Endovasc. Surg.* **2014**, *48*, 5−17.

(4) Libby, P. Current concepts of the pathogenesis of the acute coronary syndromes. *Circulation* **2001**, *104*, 365−72.

(5) Lindon, J. C.; Nicholson, J. K. Spectroscopic and statistical techniques for information recovery in metabonomics and metabolomics. *Annu. Rev. Anal. Chem.* **2008**, *1*, 45−69.

(6) Nicholson, J. K.; Lindon, J. C.; Holmes, E. 'Metabonomics': understanding the metabolic responses of living systems to pathophysiological stimuli via multivariate statistical analysis of biological NMR spectroscopic data. *Xenobiotica* **1999**, *29*, 1181−9.

(7) Sabatine, M. S.; Liu, E.; Morrow, D. A.; Heller, E.; McCarroll, R.; Wiegand, R.; Berriz, G. F.; Roth, F. P.; Gerszten, R. E. Metabolomic identification of novel biomarkers of myocardial ischemia. *Circulation* **2005**, *112*, 3868−75.

(8) Mayr, M.; Chung, Y. L.; Mayr, U.; Yin, X.; Ly, L.; Troy, H.; Fredericks, S.; Hu, Y.; Griffiths, J. R.; Xu, Q. Proteomic and metabolomic analyses of atherosclerotic vessels from apolipoprotein E-deficient mice reveal alterations in inflammation, oxidative stress, and energy metabolism. *Arterioscler., Thromb., Vasc. Biol.* **2005**, *25*, 2135−42.

(9) Trupp, M.; Zhu, H.; Wikoff, W. R.; Baillie, R. A.; Zeng, Z. B.; Karp, P. D.; Fiehn, O.; Krauss, R. M.; Kaddurah-Daouk, R. Metabolomics reveals amino acids contribute to variation in response to simvastatin treatment. *PLoS One* **2012**, *7*, e38386.

(10) Yerges-Armstrong, L. M.; Ellero-Simatos, S.; Georgiades, A.; Zhu, H.; Lewis, J. P.; Horenstein, R. B.; Beitelshees, A. L.; Dane, A.; Reijmers, T.; Hankemeier, T.; Fiehn, O.; Shuldiner, A. R.; Kaddurah-Daouk, R. Purine pathway implicated in mechanism of resistance to aspirin therapy: pharmacometabolomics-informed pharmacogenomics. *Clin. Pharmacol. Ther.* **2013**, *94*, 525−32.

(11) Yap, I. K.; Brown, I. J.; Chan, Q.; Wijeyesekera, A.; Garcia-Perez, I.; Bictash, M.; Loo, R. L.; Chadeau-Hyam, M.; Ebbels, T.; De Iorio, M.; Maibaum, E.; Zhao, L.; Kesteloot, H.; Daviglus, M. L.; Stamler, J.; Nicholson, J. K.; Elliott, P.; Holmes, E. Metabolome-wide association study identifies multiple biomarkers that discriminate north and south Chinese populations at differing risks of cardiovascular disease: INTERMAP study. *J. Proteome Res.* **2010**, *9*, 6647−54.

(12) Yu, B.; Zheng, Y.; Alexander, D.; Manolio, T. A.; Alonso, A.; Nettleton, J. A.; Boerwinkle, E. Genome-wide association study of a heart failure related metabolomic profile among African Americans in the Atherosclerosis Risk in Communities (ARIC) study. *Genet. Epidemiol.* **2013**, *37*, 840−5.

(13) Walsh, M. C.; McLoughlin, G. A.; Roche, H. M.; Ferguson, J. F.; Drevon, C. A.; Saris, W. H.; Lovegrove, J. A.; Riserus, U.; Lopez-Miranda, J.; Defoort, C.; Kiec-Wilk, B.; Brennan, L.; Gibney, M. J. Impact of geographical region on urinary metabolomic and plasma fatty acid profiles in subjects with the metabolic syndrome across Europe: the LIPGENE study. *Br. J. Nutr.* **2014**, *111*, 424−31.

(14) Ciborowski, M.; Martin-Ventura, J. L.; Meilhac, O.; Michel, J. B.; Ruperez, F. J.; Tunon, J.; Egido, J.; Barbas, C. Metabolites secreted by human atherothrombotic aneurysms revealed through a metabolomic approach. *J. Proteome Res.* **2011**, *10*, 1374−82.

(15) Stegemann, C.; Drozdov, I.; Shalhoub, J.; Humphries, J.; Ladroue, C.; Didangelos, A.; Baumert, M.; Allen, M.; Davies, A. H.; Monaco, C.; Smith, A.; Xu, Q.; Mayr, M. Comparative lipidomics profiling of human atherosclerotic plaques. *Circ. Cardiovasc. Genet.* **2011**, *4*, 232−42.

(16) Bianda, N.; Di Valentino, M.; Periat, D.; Segatto, J. M.; Oberson, M.; Moccetti, M.; Sudano, I.; Santini, P.; Limoni, C.; Froio, A.; Stuber, M.; Corti, R.; Gallino, A.; Wyttenbach, R. Progression of human carotid and femoral atherosclerosis: a prospective follow-up study by magnetic resonance vessel wall imaging. *Eur. Heart J.* **2012**, *33*, 230−7.

(17) Herisson, F.; Heymann, M. F.; Chetiveaux, M.; Charrier, C.; Battaglia, S.; Pilet, P.; Rouillon, T.; Krempf, M.; Lemarchand, P.; Heymann, D.; Goueffic, Y. Carotid and femoral atherosclerotic plaques show different morphology. *Atherosclerosis* **2011**, *216*, 348−54.

(18) Shaikh, S.; Brittenden, J.; Lahiri, R.; Brown, P. A.; Thies, F.; Wilson, H. M. Macrophage subtypes in symptomatic carotid artery and femoral artery plaques. *Eur. J. Vasc. Endovasc. Surg.* **2012**, *44*, 491−7.

(19) Gavaghan, C. L.; Holmes, E.; Lenz, E.; Wilson, I. D.; Nicholson, J. K. An NMR-based metabonomic approach to investigate the biochemical consequences of genetic strain differences: application to the C57BL10J and Alpk:ApfCD mouse. *FEBS Lett.* **2000**, *484*, 169−74.

(20) Vorkas, P. A.; Giorgis, I.; Muzaffar, A. A.; Davies, A. H.; Want, E. J.; Holmes, E. Untargeted UPLC-MS profiling pipeline to expand tissue metabolome coverage: Application to cardiovascular disease. *Anal. Chem.* **2015**, in press. DOI: 10.1021/ac503775m.

(21) Gika, H. G.; Theodoridis, G. A.; Wingate, J. E.; Wilson, I. D. Within-day reproducibility of an HPLC−MS-based method for metabonomic analysis: application to human urine. *J. Proteome Res.* **2007**, *6*, 3291−303.

(22) Eriksson, L.; Trygg, J.; Wold, S. CV-ANOVA for significance testing of PLS and OPLS® models. *J. Chemom.* **2008**, *22*, 594−600.

(23) Holmes, E.; Loo, R. L.; Stamler, J.; Bictash, M.; Yap, I. K.; Chan, Q.; Ebbels, T.; De Iorio, M.; Brown, I. J.; Veselkov, K. A.; Daviglus, M. L.; Kesteloot, H.; Ueshima, H.; Zhao, L.; Nicholson, J. K.; Elliott, P. Human metabolic phenotype diversity and its association with diet and blood pressure. *Nature* **2008**, *453*, 396−400.

(24) Legido-Quigley, C.; McDermott, L.; Vilca-Melendez, H.; Murphy, G. M.; Heaton, N.; Lindon, J. C.; Nicholson, J. K.; Holmes, E. Bile UPLC−MS fingerprinting and bile acid fluxes during human liver transplantation. *Electrophoresis* **2011**, *32*, 2063−70.

(25) Cotter, D.; Maer, A.; Guda, C.; Saunders, B.; Subramaniam, S. LMPD: LIPID MAPS proteome database. *Nucleic Acids Res.* **2006**, *34*, D507−10.

(26) Wishart, D. S.; Knox, C.; Guo, A. C.; Eisner, R.; Young, N.; Gautam, B.; Hau, D. D.; Psychogios, N.; Dong, E.; Bouatra, S.; Mandal, R.; Sinelnikov, I.; Xia, J.; Jia, L.; Cruz, J. A.; Lim, E.; Sobsey, C. A.; Shrivastava, S.; Huang, P.; Liu, P.; Fang, L.; Peng, J.; Fradette, R.; Cheng, D.; Tzur, D.; Clements, M.; Lewis, A.; De Souza, A.; Zuniga, A.; Dawe, M.; Xiong, Y.; Clive, D.; Greiner, R.; Nazyrova, A.; Shaykhutdinov, R.; Li, L.; Vogel, H. J.; Forsythe, I. HMDB: a knowledgebase for the human metabolome. *Nucleic Acids Res.* **2009**, *37*, D603−10.

(27) Smith, C. A.; O'Maille, G.; Want, E. J.; Qin, C.; Trauger, S. A.; Brandon, T. R.; Custodio, D. E.; Abagyan, R.; Siuzdak, G. METLIN: a metabolite mass spectral database. *Ther. Drug Monit.* **2005**, *27*, 747−51.

(28) Spagou, K.; Wilson, I. D.; Masson, P.; Theodoridis, G.; Raikos, N.; Coen, M.; Holmes, E.; Lindon, J. C.; Plumb, R. S.; Nicholson, J. K.; Want, E. J. HILIC−UPLC−MS for exploratory urinary metabolic profiling in toxicological studies. *Anal. Chem.* **2011**, *83*, 382−90.

(29) Kanehisa, M.; Goto, S. KEGG: Kyoto Encyclopedia of Genes and Genomes. *Nucleic Acids Res.* **2000**, *28*, 27−30.

(30) Wilson, I. D.; Nicholson, J. K.; Castro-Perez, J.; Granger, J. H.; Johnson, K. A.; Smith, B. W.; Plumb, R. S. High resolution "ultra performance" liquid chromatography coupled to oa-TOF mass spectrometry as a tool for differential metabolic pathway profiling in functional genomic studies. *J. Proteome Res.* **2005**, *4*, 591−8.

(31) Fahy, E.; Subramaniam, S.; Murphy, R. C.; Nishijima, M.; Raetz, C. R.; Shimizu, T.; Spener, F.; van Meer, G.; Wakelam, M. J.; Dennis, E. A. Update of the LIPID MAPS comprehensive classification system for lipids. *J. Lipid Res.* **2009**, *50*, S9−14.

(32) Griffin, J. L.; Atherton, H.; Shockcor, J.; Atzori, L. Metabolomics as a tool for cardiac research. *Nat. Rev. Cardiol.* **2011**, *8*, 630−43.

(33) Radovic, B.; Aflaki, E.; Kratky, D. Adipose triglyceride lipase in immune response, inflammation, and atherosclerosis. *Biol. Chem.* **2012**, *393*, 1005−11.

DOI: 10.1021/pr5009898
J. Proteome Res. 2015, 14, 1389−1399

(34) Catala, A. A synopsis of the process of lipid peroxidation since the discovery of the essential fatty acids. *Biochem. Biophys. Res. Commun.* **2010**, *399*, 318−23.
(35) Mackness, M. I.; Durrington, P. N. HDL, its enzymes and its potential to influence lipid peroxidation. *Atherosclerosis* **1995**, *115*, 243−53.
(36) Leonarduzzi, G.; Gamba, P.; Gargiulo, S.; Biasi, F.; Poli, G. Inflammation-related gene expression by lipid oxidation-derived products in the progression of atherosclerosis. *Free Radical Biol. Med.* **2012**, *52*, 19−34.
(37) Leitinger, N. Cholesteryl ester oxidation products in atherosclerosis. *Mol. Aspects Med.* **2003**, *24*, 239−50.
(38) Hutchins, P. M.; Moore, E. E.; Murphy, R. C. Electrospray MS/MS reveals extensive and nonspecific oxidation of cholesterol esters in human peripheral vascular lesions. *J. Lipid Res.* **2011**, *52*, 2070−83.
(39) Fillios, L. C.; Naito, C.; Andrus, S. B.; Roach, A. M. The hypercholesteremic and atherogenic properties of various purines and pyrimidines. *Am. J. Clin. Nutr.* **1959**, *7*, 70−5.
(40) Ralevic, V.; Burnstock, G. Effects of purines and pyrimidines on the rat mesenteric arterial bed. *Circ. Res.* **1991**, *69*, 1583−90.
(41) Burnstock, G. Control of vascular tone by purines and pyrimidines. *Br. J. Pharmacol.* **2010**, *161*, 527−9.
(42) Cronstein, B. N. Adenosine, an endogenous anti-inflammatory agent. *J. Appl. Physiol.* **1994**, *76*, 5−13.
(43) da Rocha Lapa, F.; da Silva, M. D.; de Almeida Cabrini, D.; Santos, A. R. Anti-inflammatory effects of purine nucleosides, adenosine and inosine, in a mouse model of pleurisy: evidence for the role of adenosine A2 receptors. *Purinergic Signalling* **2012**, *8*, 693−704.
(44) Quemeneur, L.; Gerland, L. M.; Flacher, M.; Ffrench, M.; Revillard, J. P.; Genestier, L. Differential control of cell cycle, proliferation, and survival of primary T lymphocytes by purine and pyrimidine nucleotides. *J. Immunol* **2003**, *170*, 4986−95.
(45) Chatterjee, S. Sphingolipids in atherosclerosis and vascular biology. *Arterioscler., Thromb., Vasc. Biol.* **1998**, *18*, 1523−33.
(46) Bismuth, J.; Lin, P.; Yao, Q.; Chen, C. Ceramide: a common pathway for atherosclerosis? *Atherosclerosis* **2008**, *196*, 497−504.
(47) Taha, T. A.; Mullen, T. D.; Obeid, L. M. A house divided: ceramide, sphingosine, and sphingosine-1-phosphate in programmed cell death. *Biochim. Biophys. Acta* **2006**, *1758*, 2027−36.
(48) Portman, O. W.; Alexander, M. Metabolism of sphingolipids by normal and atherosclerotic aorta of squirrel monkeys. *J. Lipid Res.* **1970**, *11*, 23−30.
(49) Prokazova, N. V.; Bergelson, L. D. Gangliosides and atherosclerosis. *Lipids* **1994**, *29*, 1−5.
(50) Merrill, A. H., Jr. Sphingolipid and glycosphingolipid metabolic pathways in the era of sphingolipidomics. *Chem. Rev.* **2011**, *111*, 6387−422.
(51) Vacaru, A. M.; Tafesse, F. G.; Ternes, P.; Kondylis, V.; Hermansson, M.; Brouwers, J. F.; Somerharju, P.; Rabouille, C.; Holthuis, J. C. Sphingomyelin synthase-related protein SMSr controls ceramide homeostasis in the ER. *J. Cell Biol.* **2009**, *185*, 1013−27.
(52) Ichi, I.; Nakahara, K.; Miyashita, Y.; Hidaka, A.; Kutsukake, S.; Inoue, K.; Maruyama, T.; Miwa, Y.; Harada-Shiba, M.; Tsushima, M.; Kojo, S. Association of ceramides in human plasma with risk factors of atherosclerosis. *Lipids* **2006**, *41*, 859−63.
(53) Grandl, M.; Bared, S. M.; Liebisch, G.; Werner, T.; Barlage, S.; Schmitz, G. E-LDL and Ox-LDL differentially regulate ceramide and cholesterol raft microdomains in human macrophages. *Cytometry, Part A* **2006**, *69*, 189−91.
(54) Ridgway, N. D.; Byers, D. M.; Cook, H. W.; Storey, M. K. Integration of phospholipid and sterol metabolism in mammalian cells. *Prog. Lipid Res.* **1999**, *38*, 337−60.
(55) Seimon, T.; Tabas, I. Mechanisms and consequences of macrophage apoptosis in atherosclerosis. *J. Lipid Res.* **2009**, *50*, S382−7.
(56) Yao, P. M.; Tabas, I. Free cholesterol loading of macrophages induces apoptosis involving the fas pathway. *J. Biol. Chem.* **2000**, *275*, 23807−13.
(57) Tafesse, F. G.; Vacaru, A. M.; Bosma, E. F.; Hermansson, M.; Jain, A.; Hilderink, A.; Somerharju, P.; Holthuis, J. C. Sphingomyelin synthase-related protein SMSr is a suppressor of ceramide-induced mitochondrial apoptosis. *J. Cell Sci.* **2014**, *127*, 445−54.
(58) Yanes, O.; Clark, J.; Wong, D. M.; Patti, G. J.; Sanchez-Ruiz, A.; Benton, H. P.; Trauger, S. A.; Desponts, C.; Ding, S.; Siuzdak, G. Metabolic oxidation regulates embryonic stem cell differentiation. *Nat. Chem. Biol.* **2010**, *6*, 411−7.
(59) Bunn, R. C.; Cockrell, G. E.; Ou, Y.; Thrailkill, K. M.; Lumpkin, C. K., Jr.; Fowlkes, J. L. Palmitate and insulin synergistically induce IL-6 expression in human monocytes. *Cardiovasc. Diabetol.* **2010**, *9*, 73.
(60) Boren, J.; Brindle, K. M. Apoptosis-induced mitochondrial dysfunction causes cytoplasmic lipid droplet formation. *Cell Death Differ.* **2012**, *19*, 1561−70.
(61) Dromparis, P.; Michelakis, E. D. Mitochondria in vascular health and disease. *Annu. Rev. Physiol.* **2013**, *75*, 95−126.
(62) Chandak, P. G.; Radovic, B.; Aflaki, E.; Kolb, D.; Buchebner, M.; Frohlich, E.; Magnes, C.; Sinner, F.; Haemmerle, G.; Zechner, R.; Tabas, I.; Levak-Frank, S.; Kratky, D. Efficient phagocytosis requires triacylglycerol hydrolysis by adipose triglyceride lipase. *J. Biol. Chem.* **2010**, *285*, 20192−201.

DOI: 10.1021/pr5009898
J. Proteome Res. 2015, 14, 1389−1399